Calculated electrical conductivity and thermopower of silver-palladium alloys

W. H. Butler and G. M. Stocks
Metals and Ceramics Division, Oak Ridge National Laboratory, Oak Ridge, Tennessee 37830
(Received 28 November 1983)

The electronic structures of Ag_xPd_{1-x} alloys were calculated by using a charge self-consistent version of the Korringa-Kohn-Rostoker coherent-potential approximation. The results of these calculations were then used to calculate the low-temperature electrical resistivity and the diffusion thermopower of the alloys. Excellent agreement with experiment was obtained for the magnitude and composition variation of the resistivity and the thermopower. The calculation used no adjustable parameters. The only experimental inputs were the atomic numbers of silver and palladium and the alloy lattice spacings.

I. INTRODUCTION

The silver-palladium alloy system occupies a special place in the history of alloy theory and band theory. It was in the context of a study of this system that Mott, in 1935, introduced the *rigid-band* model to describe the electronic structure of alloys and the *s-d* model to describe the electronic structure of transition metals.[1] These models have been especially durable because they provide simple pictures that relate directly to experiments on real materials.

The present paper presents the results of first-principles calculations of the conductivity and thermopower of Ag_xPd_{1-x} alloys. In these calculations the *s-d* and rigid-band models have been replaced by the self-consistent-field Korringa-Kohn-Rostoker coherent-potential-approximation (SCF KKR CPA).[2] The results of the calculations support some of Mott's early ideas. It is found that the energy bands near the Fermi energy maintain their integrity in these alloys so that a *common* band model can be used to discuss transport. In addition, one band which crosses the Fermi energy has a relatively high group velocity while the group velocities of the other bands are much lower. These bands correspond, respectively, to the *s* and *d* electrons in Mott's *s-d* model.

The disagreements, especially in detail, between the present results and the early models are also quite significant. We find, for example, that the fast electrons (the *s* electrons of the *s-d* model) have predominantly *d* character in the palladium-rich alloys. As might be expected, the common bands of the alloy differ considerably from rigid bands based either on palladium or silver. Our explanation for the striking asymmetry in the resistivity-versus-concentration curves is also different from that of Mott.

In Sec. II of this paper we describe the calculations. Section III contains a discussion of the results. A preliminary account of this work has appeared previously.[3]

II. CALCULATION OF THE ELECTRICAL CONDUCTIVITY OF Ag_xPd_{1-x} ALLOYS

The calculations described in this section are based on a very simple version of transport theory. The electrical conductivity is calculated from

$$\sigma=\frac{2e^2}{3(2\pi)^3}\int_{\epsilon_F}\frac{dS_k}{\hbar v_k}v_k^2\tau_k\ , \tag{1}$$

where the integral is over the alloy Fermi surface, and v_k and τ_k are, respectively, the electronic velocities and lifetimes. The use of such a formula assumes at the very least that alloy energy bands are well defined. The discerning reader will also notice that Eq. (1) neglects the "scattering-in" term of the Boltzmann equation, or, in Green's-function language, the "vertex corrections." It will be shown that these are valid approximations for the calculation of the transport properties of Ag_xPd_{1-x} alloys. They are probably valid in many other transition-metal alloy systems as well.

The most important step in calculating transport properties is the obtainment of an adequate approximation for the electronic structure of the system. The calculations reported here are based on a muffin-tin model of the alloy. In this model the crystal potential is imagined to consist of an array of nonoverlapping spherical potentials. These potentials are arranged periodically in space (e.g., on a fcc lattice), but the type of potential on a given site is random. A given site may be occupied by a silver potential (with probability x) or a palladium potential (with probability $1-x$). The muffin-tin model provides a much more flexible and realistic description of alloys than the tight-binding model with only diagonal disorder which has been used in most previous alloy calculations.

The electronic structure associated with a muffin-tin alloy Hamiltonian can be calculated approximately by means of the KKR CPA.[4] This technique combines the ideas of the KKR method of band theory[5] and the CPA technique for determining approximately the electronic structure of alloys.[6] The KKR method allows one to calculate the electronic structure of a periodic muffin-tin Hamiltonian, while the CPA gives a prescription for replacing the random-alloy Hamiltonian with an approximate periodic one. The computational aspects of applying the KKR CPA to realistic systems have been described by Stocks *et al.*[7] KKR CPA calculations have also been performed by Bansil and co-workers.[8]

The ability to calculate the electronic structure associat-

ed with a given set of atomic potentials is of little use without a means of generating the appropriate atomic potentials. Recently, it has become possible to construct charge self-consistent potentials within the KKR CPA.[2] Starting with *ad hoc* guesses for the silver and palladium potentials in the alloy, the KKR CPA equations can be solved and used to determine the charge density on a silver or palladium site in the alloy. These charge densities are then used to generate new silver and palladium potentials using the local-density approximation.[9] If the new potentials differ from the original ones the KKR CPA is used again, and the process is continued until charge self-consistency is achieved.

From the KKR CPA one can calculate the alloy density of states, the local density of states for a silver or palladium site, and, of course, the charge density on a silver or palladium site. The aspect of the electronic structure most relevant to transport, however, is the Bloch spectral density $A_B(\vec{k},\epsilon)$. The correct formula for calculating this quantity within the KKR CPA was derived recently by Faulkner and Stocks.[10] The Bloch spectral density for a perfectly periodic system would be a sum of δ functions located at those values of ϵ and k which determine the dispersion relation for the crystal,

$$A_B(\vec{k},\epsilon)=\sum_n \delta(\epsilon-\epsilon_n^0(\vec{k}))\ . \tag{2}$$

When the crystal is disordered by alloying, the peaks in the spectral function are broadened, and the spectral density takes on a form similar to

$$A_B(\vec{k},\epsilon)=\frac{1}{\pi}\sum_n \frac{\Gamma_n(\vec{k})}{[\epsilon-\epsilon_n^0(\vec{k})-\Delta_n(\vec{k})]^2+\Gamma_n^2(\vec{k})}\ . \tag{3}$$

According to Eq. (3), the effect of disorder on the electronic structure is the shifting and broadening of the energy bands by amounts $\Delta_n(\vec{k})$ and $\Gamma_n(\vec{k})$, respectively. Plots of $A_B(\vec{k},\epsilon)$ as a function of energy for various values of $\vec{k}$ are shown in Ref. 2. Figure 1 shows $A_B(\vec{k},\epsilon)$ as a function of $\vec{k}$ for three concentrations. For each alloy the energy is fixed at the alloy Fermi energy. It is clear from Fig. 1 that the sheet centered at Γ maintains its integrity throughout the concentration range. The other sheets are less well defined, but they carry relatively little current (none for $x \gtrsim 0.5$). At each energy and for each direction in $\vec{k}$ space the peaks in $A_B(\vec{k},\epsilon)$ can be located. These determine the alloy band structure $\epsilon_n(\vec{k})=\epsilon_n^0(\vec{k})+\Delta_n(\vec{k})$ from which the group velocities can be determined, $\vec{v}_n(\vec{k})=\vec{\nabla}_k\epsilon_n(\vec{k})$. Similarly, the width of each peak $\Gamma_n(\vec{k})$ determines the lifetime of the state with energy ϵ and momentum $\vec{k}$, $\tau_n(\vec{k})=\hbar/\Gamma_n(\vec{k})$. Thus the spectral function provides the information needed to calculate the electrical conductivity from Eq. (1).

Thus the first step in calculating the conductivity from the results of the SCF KKR CPA was to evaluate the Bloch spectral function at the alloy Fermi energy along rays in $\vec{k}$ space emanating from the Γ point (as in Fig. 1). The peaks in the spectral function along each ray were then located numerically and fit by means of a nonlinear least-squares procedure to the function

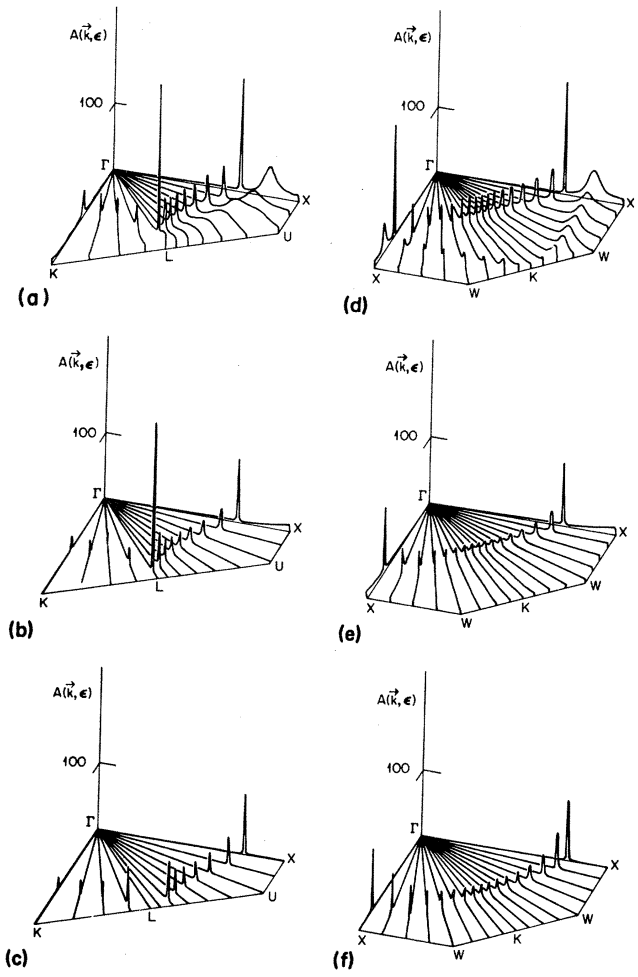

FIG. 1. Fermi-energy Bloch spectral functions in the (110) and (100) planes for Ag_xPd_{1-x} alloys. Panels (a)—(c) are for the (110) plane and silver concentrations of 0.2, 0.5, and 0.8. Panels (d)—(f) are for the (100) plane and the same silver concentrations as (a)—(c).

$$f(k)=a+bk+c/[(k-k_0)^2+\gamma^2]\ . \tag{4}$$

The adjustable parameters k_0 and γ give, respectively, the position of the peak and the width of the peak, both measured along the ray in $\vec{k}$ space. If this procedure is repeated at nearby energies, sufficient information can be obtained to construct $\epsilon(\vec{k})$, $\hbar v_k$, and τ_k, which can be used to evaluate Eq. (1).

It is also possible to calculate $\sigma(\epsilon)$ using only the information contained in the spectral density evaluated at one energy. By recognizing that $v_k\tau_k=l_k$, the mean free path, Eq. (1) can be written as

$$\sigma(\epsilon)=\frac{2e^2}{3(2\pi)^3\hbar}\int_\epsilon dS_k l_k\ , \tag{5}$$

but γ from Eq. (4) is just the projection of the mean free path along the ray. Thus if $\hat{n}$ is the normal to the surface, and $\hat{k}$ is a unit vector along the search ray, $l_k=\gamma/\hat{k}\cdot\hat{n}$. Similarly, the element of surface area subtended by a solid angle $d\Omega_k$ is $dS_k=k^2 d\Omega_k/\hat{k}\cdot\hat{n}$. Thus Eq. (5) is equivalent to

$$\sigma(\epsilon)=\frac{2e^2}{3\hbar(2\pi)^3}\int_\epsilon \frac{k^2 d\Omega_k}{(\hat{k}\cdot\hat{n})^2}\gamma_k^{-1}. \quad (6)$$

A set of rays emanating from the point Γ was defined by the mesh shown in Fig. 2(a). The mesh is in the $k_z=1$ plane. The intervals $0\le k_x\le 1$ and $0\le k_y\le 1$ in this plane are divided into n_s subintervals. In Fig. 2, $n_s=8$, but in the calculations n_s ranged from 16 to 128. Each mesh point can be labeled by two integers m and n where $0\le n\le n_s$ and $m\ge n$. The directions, defined by connecting Γ to these mesh points, define the rays used in the integration,

$$\hat{k}(m,n)=(m,n,n_s)/(m^2+n^2+n_s^2)^{1/2}. \quad (7)$$

The alloy Fermi surface is then defined by the peak position $k(m,n)$ for each ray, i.e., $\vec{k}(m,n)=k(m,n)\hat{k}(m,n)$. The normal vectors to the surface are determined from $\vec{k}(m,n)$, since

$$\hat{n}(m,n)=\vec{N}/|N|, \quad (8)$$

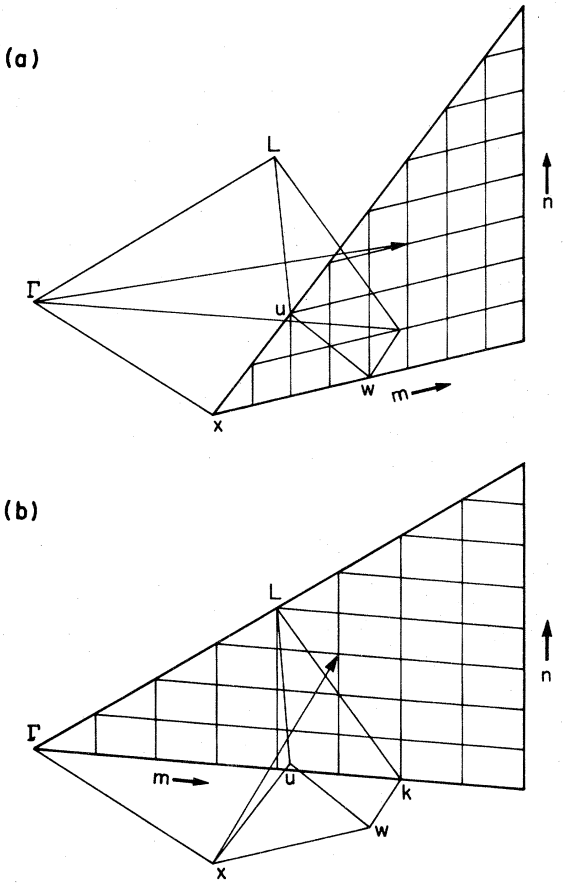

FIG. 2. (a) Mesh used to define a set of directions in $\vec{k}$ space which fill the irreducible $\frac{1}{48}$th wedge of the Brillouin zone. Directions are given in terms of integers m and n where $0\le n\le n_s$ and $m\ge n$. $\hat{k}(0,0)$ is the direction $\Gamma\to X$, $\hat{k}(n_s,0)$ is the direction $\Gamma\to K$, $\hat{k}(n_s,n_s)$ is $\Gamma\to L$, etc. (b) A mesh useful for describing surfaces centered about the X point. In this case rays emanate from X. $\hat{k}(0,0)$ is $X\to\Gamma$, $\hat{k}(n_s,0)$ is $X\to K$, and $\hat{k}(n_s,n_s)$ is $X\to L$.

where

$$\vec{N}\approx[\vec{k}(m+1,n)-\vec{k}(m-1,n)]\times[\vec{k}(m,n+1)-k(m,n-1)]. \quad (9)$$

The mesh described above works well for the Γ-centered sheet of fast electrons which carry most of the current. For the $Ag_{0.2}Pd_{0.8}$ alloy we also calculated the current carried by the flat bands centered about points X and the line joining points X and W. For this calculation rays emanating from point X to a mesh in the plane defined by the points $\vec{k}=(0,0,0)$, (1,0,1), and (1,1,1), as shown in Fig. 2(b), were used.

III. RESULTS AND DISCUSSION

A. Resistivity

The electrical resistivity calculated as described in the preceding section is shown in Fig. 3. In our opinion the agreement with experiment is excellent considering the fact that no adjustable parameters were used. The results shown in Fig. 3 differ slightly from those in Ref. 3 partly because of a refinement of the precision in performing the integral of Eq. (6), but mainly because the results in Ref. 3 contain a uniform overestimate of 6% due to a miscalculation of the numerical constants entering the resistivity formula. No other result or conclusion of Ref. 3 is affect-

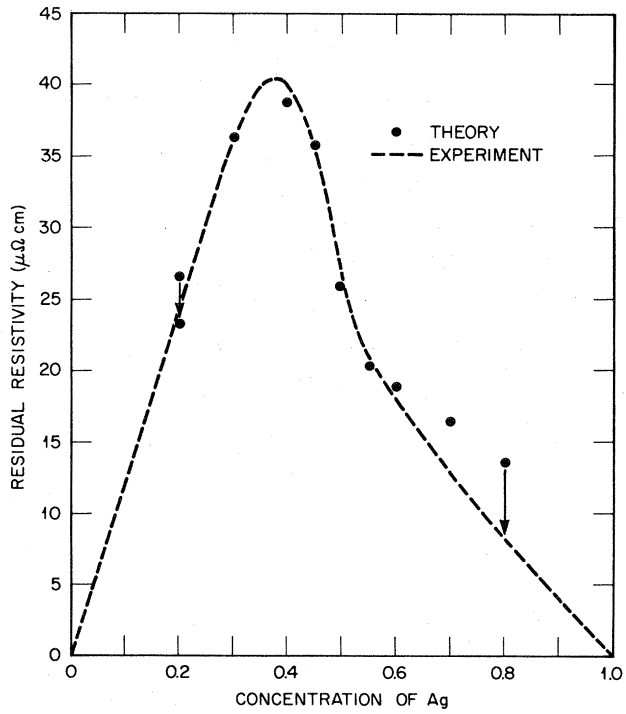

FIG. 3. Electrical resistivity of Ag_xPd_{1-x} alloys as a function of concentration. Solid circles are calculated results, and dashed line is experiment. For the $Ag_{0.2}Pd_{0.8}$ alloy, the arrow indicates the effect of including the current carried by the slow d electrons. For the $Ag_{0.8}Pd_{0.2}$ alloy the arrow indicates an *estimate* of the reduction in the resistivity which would be observed if the scattering-in term of the Boltzmann equation had not been neglected.

ed by this error.

For most of the alloys only the current carried by the Γ-centered sheet was calculated. For silver concentrations greater than or equal to 0.5 this is the only sheet, but for the palladium-rich alloys there is a large density of states associated with flat bands near the X point and in the vicinity of the line connecting the X and W points. Although these states carry the preponderance of the density of states for the palladium-rich alloys, their contribution to the current is quite modest because their velocities are so low. This is illustrated in Fig. 3 for the $Ag_{0.2}Pd_{0.8}$ alloy. The arrow shows the decrease in the resistivity due to the inclusion of the extra current carried by the slow electrons. Their contribution rapidly goes to zero as the concentration increases because both the number of states and their velocity goes to zero as the Fermi energy rises to the top of the d bands. The Fermi energy passes through the top of the d-band complex at approximately $x=0.5$.

Two essential approximations are made when the conductivity is calculated from Eqs. (1) or (6). The first approximation is the assumption that a well-defined alloy Fermi surface exists. It is clear from Fig. 1 that this is a valid approximation for these alloys. The peaks that define the states are especially well defined for the Γ-centered sheet. They are somewhat less well defined for the other states, but this does not cause a large error in the conductivity, because the total contribution of these states is so small.

The second approximation implicit in Eq. (1) is the neglect of vertex corrections or, equivalently, the scattering-in term of the Boltzmann equation. This approximation can be justified for the palladium-rich alloys when they are described by the muffin-tin Hamiltonian used here. Consider the Boltzmann equation[11]

$$\frac{e}{\hbar}\frac{\partial f_k}{\partial \epsilon_k}\vec{\mathscr{E}}\cdot\vec{\nabla}_k\epsilon_k=-\sum_{k'}P_{kk'}(g_k-g_{k'})\ . \tag{10}$$

In this equation f_k is the Fermi function, $\vec{\mathscr{E}}$ is the applied electric field, $\hbar^{-1}\vec{\nabla}_k\epsilon_k$ is the Fermi velocity, $P_{kk'}$ is the probability for an electron to scatter between states k and k', and g_k is the deviation function which describes the departure of the electron distribution from the Fermi function. Once Eq. (10) has been solved for g_k, the current can be calculated from

$$\vec{j}=\vec{\sigma}\cdot\vec{\mathscr{E}}=-2e\sum_k\vec{v}_k g_k\ . \tag{11}$$

The first term on the right-hand side (rhs) of Eq. (10) is often called the "scattering-out" term because $g_k\sum_{k'}P_{kk'}$ gives the rate at which electrons are scattered *out of* state k. The second term is called the scattering-in term because $\sum_{k'}P_{kk'}g_{k'}$ gives the rate of scattering *into* state k. The scattering-out term is easily evaluated in terms of the electron lifetime since

$$\sum_{k'}P_{kk'}=1/\tau_k\ . \tag{12}$$

If the scattering-in term can be neglected in Eq. (10), we have [using Eq. (12)]

$$g_k=-e\frac{\partial f_k}{\partial \epsilon_k}\vec{v}_k\cdot\vec{\mathscr{E}}\tau_k \tag{13}$$

and

$$\vec{j}=2e^2\sum_k\frac{\partial f_k}{\partial \epsilon_k}\vec{v}_k\vec{v}_k\cdot\vec{\mathscr{E}}\tau_k\ , \tag{14}$$

from which Eq. (1) follows on the assumptions of cubic symmetry, and that $-\partial f_k/\partial\epsilon_k\simeq\delta(\epsilon_k-\epsilon_F)$.

In order to estimate the relative magnitude of the scattering-in and scattering-out terms let us assume the following form for g_k:

$$g_k=-e\vec{v}_k\cdot\vec{\mathscr{E}}\frac{\partial f}{\partial \epsilon_k}\bar{\tau}\ . \tag{15}$$

This ansatz which is sometimes called the lowest-order variational approximation[12] is identical to Eq. (13) except that the k dependence of τ is neglected and $\bar{\tau}$ may be interpreted as a variational parameter chosen so as to maximize the current. We now substitute Eq. (15) into the Boltzmann equation (10), this time keeping both terms on the rhs of Eq. (10), and we obtain

$$v_{kx}\frac{\partial f}{\partial \epsilon_k}=\sum_{k'}P_{kk'}(v_{kx}-v_{k'x})\frac{\partial f}{\partial \epsilon_k}\bar{\tau}\ , \tag{16}$$

where we have assumed the applied field to be in the x direction. Multiplying both sides of Eq. (16) by v_{kx}, summing over k, and solving for $1/\bar{\tau}$, we obtain

$$\frac{1}{\bar{\tau}}=\left[\frac{1}{\tau}\right]^{\text{out}}-\left[\frac{1}{\tau}\right]^{\text{in}}\ , \tag{17}$$

$$\left[\frac{1}{\tau}\right]^{\text{out}}=\frac{\int\frac{dS_k}{v_k}v_k^2\tau_k^{-1}}{\int\frac{dS_k}{v_k}v_k^2}\ , \tag{18}$$

$$\left[\frac{1}{\tau}\right]^{\text{in}}=\frac{\sum_{kk'}P_{kk'}\vec{v}_k\cdot\vec{v}_{k'}\left[-\frac{\partial f}{\partial \epsilon_k}\right]}{\sum_k v_k^2\left[-\frac{\partial f}{\partial \epsilon_k}\right]}\ . \tag{19}$$

Clearly, if the scattering described by $P_{kk'}$ is primarily "forward" scattering, $P_{kk'}\sim\delta_{kk'}\tau_k^{-1}$, we have $(1/\tau)^{\text{in}}\sim(1/\tau)^{\text{out}}$ On the other hand, if the scattering is completely isotropic so that $P_{kk'}$ is independent of k and k', $(1/\tau)^{\text{in}}=0$. Whichever of these two limits is closer to reality will vary from system to system. If ΔV is the (weak) potential fluctuation caused by an impurity atom,[13] $P_{kk'}$ can be approximated by

$$P_{kk'}=\frac{2\pi n}{\hbar}|\langle k|\Delta V|k'\rangle|^2\delta(\epsilon_k-\epsilon_{k'})\ , \tag{20}$$

where n is the number of impurity atoms.

If this potential fluctuation has a long range and varies slowly, forward scattering will dominate, and the scattering-in contribution to the total scattering rate will almost cancel the scattering-out contribution. Examples of this situation are long-wavelength phonons and lattice defects which extend over many lattice sites. On the other hand, if the potential fluctuation is restricted to a region which is small compared to the distance over which the

phase of the wave function changes appreciably, $(1/\tau)^{\text{in}}$ will be small. We believe that the latter case occurs in the palladium-rich alloys. These alloys have a high Fermi-energy state density which rapidly screens out potential fluctuations. In addition, most of the valence charge density is associated with the d states which are particularly tightly bound in silver and palladium. In any event, the single-site CPA precludes potential fluctuations that extend beyond a single Wigner-Seitz cell.

The scattering-in term vanishes identically in the single-band tight-binding model which is used for most CPA calculations,[14] and Brouers and Verdyayev[15] suggest that it is also negligible for their multiband tight-binding model. For Hamiltonians more realistic than tight binding the scattering-in term is generally nonzero. The CPA calculations described in this paper are based on a muffin-tin Hamiltonian with KKR-type wave functions,

$$|\vec{k}\rangle=\sum_{l,m} i^l C_{lm}(\vec{k})R_l(r)Y_{lm}(\hat{r}) . \tag{21}$$

For this type of Hamiltonian Eq. (20) becomes

$$P_{kk'}=(2\pi n/\hbar)\sum_{l,m}\sum_{l',m'} C_{lm}(\vec{k})C_{l'm'}(\vec{k})C_{lm}(\vec{k}')C_{l'm'}(\vec{k}') \times\Delta V_l\Delta V_{l'}\delta(\epsilon_k-\epsilon_{k'}) , \tag{22}$$

where

$$\Delta V_l=\int dr\, r^2 R_l^2(r)\Delta V(r) . \tag{23}$$

The scattering-in term, $T^{\text{in}}=\sum_{k'}P_{kk'}g_{k'}$, will probably be quite small in the transition metals because the Fermi-energy wave functions have predominantly $l=2$ character. This is especially true of palladium and the palladium-rich Ag_xPd_{1-x} alloys.[2] If the wave-function character is entirely $l=2$ or even a combination of $l=2$ and 0, T^{in} will vanish exactly in this approximation because the sum

$$\sum_{k'} C_{lm}(\vec{k}')C_{l'm'}(\vec{k}')g_{k'}$$

vanishes on account of the odd parity of $g_{k'}$ and the even parity of the product $C_{lm}(k)C_{l'm'}(k)$ when l and l' are either both even or both odd. It is clear from Ref. 2 that the Fermi-energy density of states of the palladium-rich alloys has almost entirely $l=2$ character.

In the silver-rich alloys the Fermi energy density of states has a significant $l=1$ component, and consequently the scattering-in term is more important. The arrow in Fig. 3 for the $Ag_{0.8}Pd_{0.2}$ alloy indicates an estimate for the reduction in the resistivity due to inclusion of the scattering-in term. The estimate is based on a formula appropriate for a low concentration of scatterers in a noble or simple metal[16]

$$\frac{(1/\tau)^{\text{out}}-(1/\tau)^{\text{in}}}{(1/\tau)^{\text{out}}}=\frac{\sum_l (l+1)\sin^2(\Delta\eta_{l+1}-\Delta\eta_l)}{\sum_l (2l+1)\sin^2(\Delta\eta_l)} , \tag{24}$$

where $\Delta\eta_l=\eta_l^{\text{Pd}}-\eta_l^{\text{Ag}}$. For the phase shifts appropriate to $Ag_{0.8}Pd_{0.2}$ we obtain 0.63 for the ratio, Eq. (24).

The justification given above for the neglect of the scattering-in term in the palladium-rich alloys is contingent upon the assumption of a muffin-tin type of Hamiltonian. The critical assumption is that an impurity potential perturbs only one muffin tin. In reality, however, the potential fluctuation due to an impurity atom extends well beyond its Wigner-Seitz cell. In addition to perturbing the potential in neighboring cells, the impurity atom will set up a relatively long-range strain field. These small, long-ranged potential fluctuations cause substantial forward scattering. For this reason it would be a mistake to use the lifetime calculated from the KKR CPA to estimate the impurity-induced scattering rates observed in de Haas–van Alphen experiments (Dingle temperatures). A substantial amount of forward scattering is missing from the KKR CPA inverse lifetimes with the consequence that the Dingle temperatures are underestimated. The KKR CPA lifetimes work well for calculating the electrical resistivity, however, because the forward scattering does not enter that quantity.

In order to illustrate this point, the averages of τ^{-1} over the Fermi surface were used to calculate Dingle temperatures for the $Ag_{0.2}Pd_{0.8}$ and $Ag_{0.8}Pd_{0.2}$ alloys using the formula

$$X_D=\frac{\hbar\langle\tau^{-1}\rangle}{2\pi(1+\lambda)k_B} . \tag{25}$$

For the $Ag_{0.2}Pd_{0.8}$ alloy the calculated Dingle temperature is approximately 7.4 K/at.%, 25% less than the experimental value of 10 K/at.% reported by Ernest *et al.*,[17] and for the $Ag_{0.8}Pd_{0.2}$ alloy the calculated Dingle temperature is 9 K/at.%, less than one-third the value ($\sim$30 K/at.%) reported by Sang and Myers.[18] The values of $1+\lambda$, the estimated mass enhancements, used in the above calculations of X_D were 1.5 for the 80-at.% palladium-rich alloy and 1.2 for the silver-rich alloy.

One of the most interesting features of the resistivity of Ag_xPd_{1-x} alloys is the asymmetry of the resistivity-versus-composition curve (Fig. 3). Mott's explanation for this asymmetry in terms of the *s-d* and *rigid-band* models was an important early success of these models, which undoubtedly contributed to their rapid acceptance. Ironically, although the basic *s-d* and *rigid-band* models seem to be qualitatively valid for Ag_xPd_{1-x} alloys, it appears from our calculations that Mott's explanation for the asymmetry is not correct. The Mott explanation is simple and reasonable. From Eq. (20) the scattering rate should be given by

$$\hbar/\tau_k=2\pi n\sum_{k'}|\langle k|\Delta V|k'\rangle|^2\delta(\epsilon_F-\epsilon_{k'}) . \tag{26}$$

Since the Fermi-energy density of states is given by

$$N(\epsilon_F)=\sum_k\delta(\epsilon_F-\epsilon_k) ,$$

Eq. (26) may be written as

$$\hbar/\tau_k=2\pi n\langle(\Delta V)^2\rangle N(\epsilon_F) . \tag{27}$$

Since the density of states is much higher for the palladium-rich alloys, one would certainly expect from Eq. (27) that, for the same concentration of impurities, the

scattering rates would be higher for palladium-rich alloys than for silver-rich ones. Our calculations (Fig. 2 of Ref. 3) do not show this effect, however. The average scattering rate for $Ag_{0.8}Pd_{0.2}$ is just as high as that for $Ag_{0.2}Pd_{0.8}$. We find that the asymmetry in the resistivity curve comes primarily from the higher Fermi velocity of the s electrons in silver, and secondarily from the greater importance of vertex corrections in the silver-rich alloys.

The fallacy in Mott's argument lies in the use of Eq. (20) for the scattering probability. The scattering by the potential fluctuation is sufficiently strong that its effect on the wave functions must be included. This is accomplished according to the theory of substitutional impurities[19] by replacing ΔV by the proper t matrix in Eq. (20),

$$P_{kk'}=\frac{2\pi n}{\hbar}\,|\,T_{kk'}\,|^2\,\delta(\epsilon_k-\epsilon_{k'})\ , \tag{28}$$

where $T_{kk'}$ is given (using the KKR formalism) by

$$T_{kk'}=\sum_{l,m} C_{lm}(\vec{k})C_{lm}(\vec{k}')S_{lm}\ , \tag{29}$$

$$S_{lm}=\frac{1}{\sqrt{E}}\Delta\cot\eta_l/[1+\Delta\cot(\eta_l)\tilde{\tau}_{lm}]\ , \tag{30}$$

$$\Delta\cot\eta_l=\cot\eta_l^i-\cot\eta_l^h\ , \tag{31}$$

$$\tilde{\tau}=\frac{-\sqrt{E}}{\Omega_{BZ}}\int d^3q[t^{-1}-G'(q,\epsilon)]^{-1}\ . \tag{32}$$

Here, $\Delta\cot\eta_l$ is the difference between the cotangents of the phase shift of the impurity and that of the host, and $\tilde{\tau}_{lm}$ is the Brillouin-zone (BZ) integral of the inverse of the KKR matrix which is diagonal in the angular momentum indices for cubic systems if $l\leq 2$. The form of Eq. (29) insures that our previous conclusions concerning the smallness of the scattering-in term of the Boltzmann equation remain valid. On the other hand, the scattering rate calculated from Eq. (29),

$$\hbar/\tau_k=-n\ \mathrm{Im}T_{kk}=-n\sum_{l,m}C_{lm}^2(k)\mathrm{Im}S_{lm}\ , \tag{33}$$

is no longer necessarily proportional to the density of final states. Only if $|\,\Delta\cot(\eta_l)\tilde{\tau}_{lm}\,|\ll 1$ will Eqs. (33) and (26) be equivalent.

B. Diffusion thermopower

If a temperature gradient is set up in a conductor it will generally be accompanied by an induced electric field $\mathscr{E}$. The ratio of this field to the applied thermal gradient is called the thermopower,[20]

$$S=\frac{\mathscr{E}}{dT/dx}\ . \tag{34}$$

There are two basic causes of this induced electric field. In relatively pure systems in which the phonons have a relatively long mean free path, a nonequilibrium distribution of phonons will carry part of the thermal current. These phonons may then impart some of their momentum to the electrons via the electron-phonon interaction. This "phonon-drag" effect is not very important in concentrated Ag_xPd_{1-x} alloys because there is sufficient phonon-impurity scattering to maintain the phonon distribution function in equilibrium.

The second contribution to the thermopower arises from the fact that electrons diffusing in a thermal gradient will carry a small electrical current if the electronic structure of the metal is energy dependent in the vicinity of the Fermi energy. If the total electric current is zero (because the circuit is open) there must be an induced electric field to oppose the electrical current caused by the thermal gradient. This diffussion thermopower is given by[21]

$$S=\frac{\pi^2}{3}\frac{k^2T}{e}\frac{1}{\sigma(\epsilon_F)}\left[d\epsilon\frac{d\sigma(\epsilon)}{d\epsilon}\right]_{\epsilon_F}\ . \tag{35}$$

We have evaluated the diffusion thermopower using Eq. (35) with $\sigma(\epsilon)$ determined by Eq. (6). The results are shown in Fig. 4, where they are compared with the experimental results of Guénault.[22] The most obvious feature in the thermopower is the peak at $x=0.5$. This peak originates in the rapid energy dependence of the electron scattering rate at the top of the d-band complex. From Eq. (6) the thermopower can be written as

$$\frac{S}{T}=\frac{\pi^2}{3}\frac{k_B^2}{e}\frac{\int\frac{d\Omega_k}{(\hat{k}\cdot\hat{n})^2}\frac{k^2}{\gamma_k}\left[\frac{2}{k}\frac{dk}{d\epsilon}-\frac{1}{\gamma_k}\frac{d\gamma_k}{d\epsilon}\right]_{\epsilon_F}}{\int\frac{d\Omega_k}{(\hat{k}\cdot\hat{n})^2}\frac{k^2}{\gamma_k}} \tag{36}$$

or

$$\frac{S}{T}=\frac{\pi^2}{3}\frac{k_B^2}{e}\left[2\left\langle\frac{1}{k}\frac{dk}{d\epsilon}\right\rangle-\left\langle\frac{1}{\gamma}\frac{d\gamma}{\epsilon}\right\rangle\right]\ . \tag{37}$$

The second term on the rhs of Eq. (37) is dominant. For $x<0.5$, γ_k is largely determined by the rate of scattering from the fast (s) sheet to the slow (d) sheets. As the d

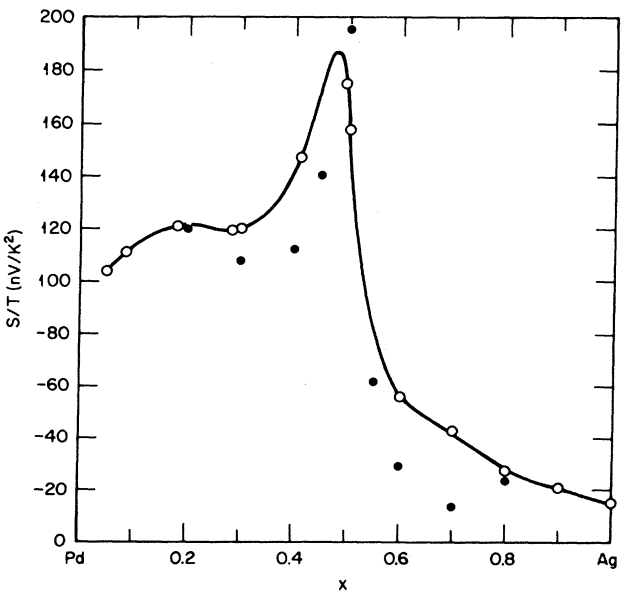

FIG. 4. Calculated (solid circles) and experimental (open circles) values of the diffusion thermopower for Ag_xPd_{1-x} alloys. The line through the experimental points is a guide for the eye.

sheets disappear at $x=0.5$ there is an abrupt decrease in γ_k and hence a large peak in S/T.

IV. CONCLUSIONS

The KKR CPA appears to be able to generate the electronic structure of alloys sufficiently well to allow the calculation of transport properties from first principles. It is highly desirable that the calculations be done with charge self-consistent potentials. An earlier resistivity calculation[23] carried out with non-self-consistent potentials gave resistivities that were too large by about 30%.

The vertex corrections are probably small in the KKR CPA for transition-metal alloys. This result should simplify transport calculations in transition-metal alloys. The surprisingly good results reported here for the thermopower indicate that the CPA represents the top of the d band well for this alloy system.

ACKNOWLEDGMENTS

This research was sponsored by the Division of Materials Sciences, U.S. Department of Energy, under Contract No. W-7405-eng-26 with the Union Carbide Corporation.

[1]N. F. Mott, Proc. Phys. Soc. London 47, 571 (1935); N. F. Mott and H. Jones, *The Theory of the Properties of Metals and Alloys* (Dover, New York, 1958), p. 300.
[2]H. Winter and G. M. Stocks, Phys. Rev. B 27, 882 (1983).
[3]G. M. Stocks and W. H. Butler, Phys. Rev. Lett. 48, 55 (1982).
[4]P. Soven, Phys. Rev. B 2, 4715 (1970); H. Shiba, Prog. Theor. Phys. 16, 77 (1971); B. L. Gyorffy, Phys. Rev. B 5, 2382 (1972).
[5]J. Korringa, Physica 8, 392 (1947); W. Kohn and N. Rostoker, Phys. Rev. 94, 1111 (1954).
[6]P. Soven, Phys. Rev. 156, 809 (1967); D. W. Taylor, *ibid.* 156, 1017 (1967).
[7]G. M. Stocks, W. M. Temmerman, and B. L. Gyorffy, in *Electrons in Disordered Metals and at Metallic Surfaces,* edited by P. Phariseau and B. L. Gyorffy (Plenum, New York, 1979), p. 193.
[8]A. Bansil, Phys. Rev. Lett. 41, 1670 (1978); R. Prasad and A. Bansil, *ibid.* 48, 113 (1982).
[9]P. Hohenberg and W. Kohn, Phys. Rev. 136, B864 (1964); W. Kohn and L. J. Sham, Phys. Rev. 140, A1133 (1965).
[10]J. S. Faulkner and G. M. Stocks, Phys. Rev. B 21, 3222 (1980).
[11]J. M. Ziman, *Electrons and Phonons* (Oxford University Press, London, 1960), p. 264.
[12]F. J. Pinski, P. B. Allen, and W. H. Butler, Phys. Rev. B 23, 5080 (1981).
[13]The arguments can be easily generalized to strong scattering and high concentrations; see Eqs. (28)—(33).
[14]B. Velický, Phys. Rev. 184, 614 (1969).
[15]F. Brouers and A. V. Vedyayev, Phys. Rev. B 2, 348 (1972).
[16]P. T. Coleridge, J. Phys. F 9, 473 (1979).
[17]D. Ernest, W. Joss, and E. Walker, in *Physics of Transition Metals, 1980,* edited by P. Rhodes (Institute of Physics, London, 1981), p. 463.
[18]D. Sang and A. Myers, J. Phys. F 6, 545 (1976).
[19]G. Lehmann, Phys. Status Solidi B 56, K33 (1983); E. Mrosan and G. Lehmann, *ibid.* 77, 607 (1976).
[20]F. J. Blatt, P. A. Schroeder, C. L. Foiles, and D. Greig, *Thermoelectric Power of Metals* (Plenum, New York, 1976).
[21]N. F. Mott and H. Jones, *The Theory of the Properties of Metals and Alloys* (Dover, New York, 1958), p. 116.
[22]A. M. Guénault, Philos. Mag. 30, 641 (1974).
[23]G. M. Stocks and W. H. Butler, in *Physics of Transition Metals, 1980,* Ref. 17, p. 467.